ELSEVIER

Journal of Power Sources 52 (1994) 201–209

JOURNAL OF POWER SOURCES

Failure mode of the negative plate in recombinant lead/acid batteries

Sven Atlung, Birgit Zachau-Christiansen

Department of Physical Chemistry-206, The Technical University, 2800 Lyngby, Denmark

Received 27 May 1994; in revised form 5 July 1994; accepted 12 July 1994

Abstract

Experimental recombinant valve-regulated lead/acid batteries failed after 250 to 350 deep cycles. The failure was attributed to the negative electrode which showed loss of capacity. When the cells were converted to operation in the flooded mode, they delivered up to 1400 deep cycles. The failure mechanism is assumed to be sulfation due to insufficient recharge. A simple model for the partial currents during recharge is used to analyse the role of recombination and hydrogen and oxygen evolution in the failure mechanism. It is concluded that, at high recombination efficiencies, hydrogen evolution prevents the complete recharge of the negative plate, thus limiting the cycle life.

Keywords: Lead/acid batteries; Failure mode; Negative plate

1. Introduction

The development of lead/acid batteries in the last decade is aimed at a number of new large-scale applications.

Among the most urgent of these are batteries for motive power, like electrical vehicles and similar traction needs. These applications require daily deep cycling. To be cost competitive, such batteries have to deliver a high amount of Wh per US $ during their lifetime.

In terms of batteries this means a large number of deep cycles, preferably 500 to 1000, before failure [1]. A high power capability and a fair energy/weight ratio is also required.

Attractive performance can be obtained in flooded tubular systems [2] and also in special flat plate systems [3,4], but there appears to be a general consensus to concentrate development on the recombinant valve-regulated lead/acid (VRLA) batteries, because they offer convenient maintenance-free operation and increased safety.

The main problem with these batteries appears to be the less satisfactory cycle life and unpredictable premature failure of the positive plate [5].

Flat plate (pasted) batteries are easier to produce than tubular batteries but, compared with these, exhibit very limited cycle life. It has been shown that this is due, to a large extent, to the degradation of the structure of the positive plate [6,7]. Cycle life can, however, be dramatically improved by exerting a high elastic pressure on the positive mass [3,4,6,8–11]. This can be achieved by modifying the traditional separator technology, by retaining the advantages of the flooded construction with free-flowing electrolyte [3,4].

Another possibility is to take advantage of the resiliency and elastic properties of the absorptive glass mat separator. This material can, by compression to 50 to 60% of its initial thickness, exert an elastic pressure of up to 100 kPa on the positive mass [11].

Using this technique, cycle lives of 1200 to 1400 deep cycles have been obtained with a total delivered energy of 140 000 to 200 000 Wh per kg positive mass [4].

The demand for maintenance-free operation is met by utilizing oxygen reduction (recombination) at the negative electrode during recharge and overcharge. This requires gas channels in the separator for transporting oxygen evolved at the positive to the negative plate. This is the case when the glass mat separator is not completely saturated with acid (starved electrolyte) [12–14].

It seems to be obvious to combine long cycle life with recombination using the compressed glass mat separator in the starved electrolyte mode.

A programme was initiated by the Danish Department of Energy to implement this technology in the Danish lead/acid battery industry, aiming at only small changes

SSDI 0378-7753(94)01963-V

in the existing production procedures. For this reason, work was based on positive and negative plates from Danish manufacturers. Further emphasis was placed on batteries suitable for use in the current Danish development of small electric vehicles [15].

2. Experimental

Cells were built with one positive and two negative plates in acrylic vessels, sealed with silicone resin and secured by bolts and nuts.

Provisions were made for throughfeeds for current and voltage connections. The cells were further provided with a Hg_2SO_4/H_2SO_4 reference electrode and a ventilation tube fitted with a low-pressure self-sealing vent.

Inner dimensions of the cells were height: 90 mm, width: 70 mm and thickness: 10–15 mm, adjusted to obtain the desired pressure on the plate packet.

Cured and formed plates were of commercial origin, negatives as well as positives machine-pasted on low antimony (2.5 wt.%) grids. The plates were very uniform in thickness and weight. The plates were cut to size retaining the lug for soldering connection wires (platinum for the positive, lead for the negative).

Plate specifications were:

(i) positives: 65 mm × 75 mm × 2 mm; active mass (PbO_2): 26–28 g, and estimated *C*/5 capacity: 3 Ah.

(ii) negatives: two plates of 60 mm × 68 mm × 1.4 mm; active mass (Pb): 2 × 14 g, and ratio Pb/PbO_2: 1.23.

The absorptive glass mat used for the separator was a commercial product, intended for VRLA batteries (Binzer) with the following specifications: thickness (non compressed): 2 mm; porosity (non compressed): 95%, and weight: 250 g/m^2.

Pore size for this type of separator is estimated at 20 to 30 μm measured perpendicular to the sheet [16].

Compressed with 70 kPa, the thickness is reduced to about 50% of the initial value. Separator sheets were cut to size 70 mm × 80 mm fitting tight into the vessel. No separate sludge space was allowed for. Sulfuric acid of sp. gr 1.28 (molality 6.25 mol/kg) was added in the desired amount.

Cycling was done with in-house built automatic equipment, controlled by an AT–PC. Discharge was always with constant current. Three specific currents were used: 48, 24 and 2.4 A per kg positive mass termed *C*/2.5, *C*/5 and *C*/50. *C*/50 to an endpoint of 1.0 V was only used for diagnostic purposes on cells approaching failure.

For *C*/5 discharges, 1.7 V was used as endpoint throughout. The *C*/2.5 discharges were either deep discharges to endpoint 1.5 V or limited discharges to 50 Ah per kg positive mass, corresponding to a depth-of-discharge of about 60% of the initial capacity.

Results are given as Ah per kg positive mass or as final voltage in the capacity limited discharges.

Charge was divided into two segments. The first segment was, as a rule, composed of a galvanostatic part until a preset cell voltage, followed by a potentiostatic part at that voltage until one of the change-over criteria to the next segment was met. The second segment had the same structure, but with different values for current and voltage. The change-over criteria could be time, minimum current, charge or charge factor.

Before the next discharge a currentless pause of at least one hour was inserted.

The equipment could be programmed to a sequence of two different discharge/charge profiles, eg., 10 *C*/2.5 discharges followed by 3 *C*/5 discharges.

Water decomposition was followed by weighing the cells and, when cells were operated in the flooded mode, water was added for about each 50th cycle.

3. Results

Fig. 1 shows the cycling behaviour of cell 9020 until cycle 400. This cell was built with 5 sheets of glass mat on each side of the positive, compressed to 5 mm interelectrode distance exerting a pressure of 70 to 80 kPa.

The cell was filled with 51 cm^3 acid of 1.28 sp. gr. corresponding stoichiometrically to 250 Ah per kg positive mass.

The cell was operated in the starved electrolyte condition, the filling of the separator pores estimated at 85%.

Discharge was 10 *C*/2.5 cycles to 1.5 V followed by 3 *C*/5 cycles to 1.7 V. Charge was 30 A per kg positive mass to 2.35 V until the current dropped to 5 A per kg positive mass followed by 5 A per kg positive mass to 2.40 V until a charge factor of 130% for the *C*/2.5

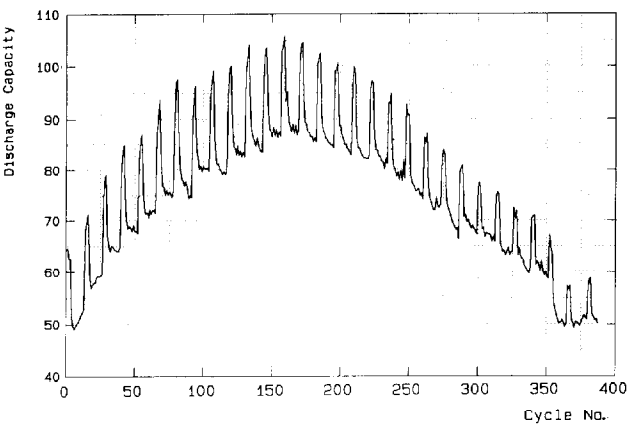

Fig. 1. Cycling of cell 9020 in the recombination mode. 10 *C*/2.5 + 3 *C*/5 discharges to 1.5 and 1.7 V, respectively. Capacities in Ah per kg positive mass.

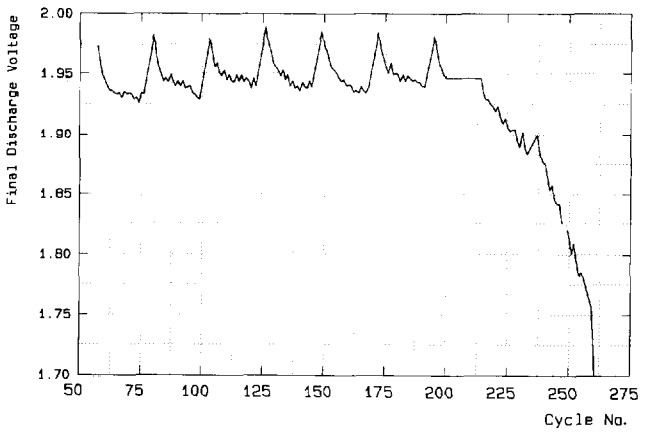

Fig. 2. Cycling of cell 9023 in the recombination mode. 20 *C*/2.5 discharges to 50 Ah per kg positive mass + 3 *C*/5 discharges to 1.7 V. Only final voltage at 50 Ah per kg positive mass is shown (*C*/2.5 current).

and 110% for the *C*/5 discharges was reached. The total charge time was 4 to 6 h.

Fig. 1 demonstrates that this cell has a limited cycle life, much below expectations. Degradation is obvious from cycle 200 and at cycle 380 when the limit of 50 Ah per kg positive mass is met. The cell delivered only 30 000 Ah per kg positive mass before failure.

Fig. 2 shows results from cell 9023. This cell was built similar to cell 9020. Discharge sequence was 10 discharges limited to 50 Ah per kg positive mass followed by 3 *C*/5 discharges to 1.7 V. The results are presented as final voltage at 50 Ah per kg positive mass. The constant endpoints – 1.7 V – for the inserted *C*/5 are omitted. (The high endpoint voltage after the *C*/5 discharges is remarkable, but not discussed in the present context.) This cell delivered only 260 cycles or about 20 000 Ah per kg positive mass before failure.

To investigate the quality of the plates used and the effect of the pressure exerted by the separator, cell 9015 was built with the same plates, as a flooded cell and with a separator configuration similar to that described in Ref. [3], which allowed the acid to circulate, and prevented recombination. The pressure was adjusted to the same value as used in the cells 9020 and 9023. The cycling history is shown in Fig. 3.

Except for a short interruption at cycle 1080, due to a corroded positive lead terminal, the cell delivered 1400 cycles and 85 000 Ah per kg positive mass before failure. This demonstrates the capability of the plates used and the pressurized concept.

Apparently, this long cycle life could not be obtained using the glass mat separator in the starved electrolyte mode.

The reason for the premature failure of the cells 9020 and 9023 was diagnosed considering the overvoltages (derived from the single electrode potentials against the reference electrode) depicted in Fig. 4 for cell 9020 at cycle 160, where the cell worked satisfactorily, compared with cycle 303, where degradation is obvious. Both cycles were *C*/2.5 to 1.5 V endpoint. It is very clear that at cycle 160 the positive is capacity limiting, whereas the negative has a sufficient capacity reserve. In cycle 303 the overvoltage of the negative is much larger, and there is a depression of the positive which may be due to a decrease in acid concentration. (With the reference electrode used, the negative rest potential is independent of acid concentration.) The

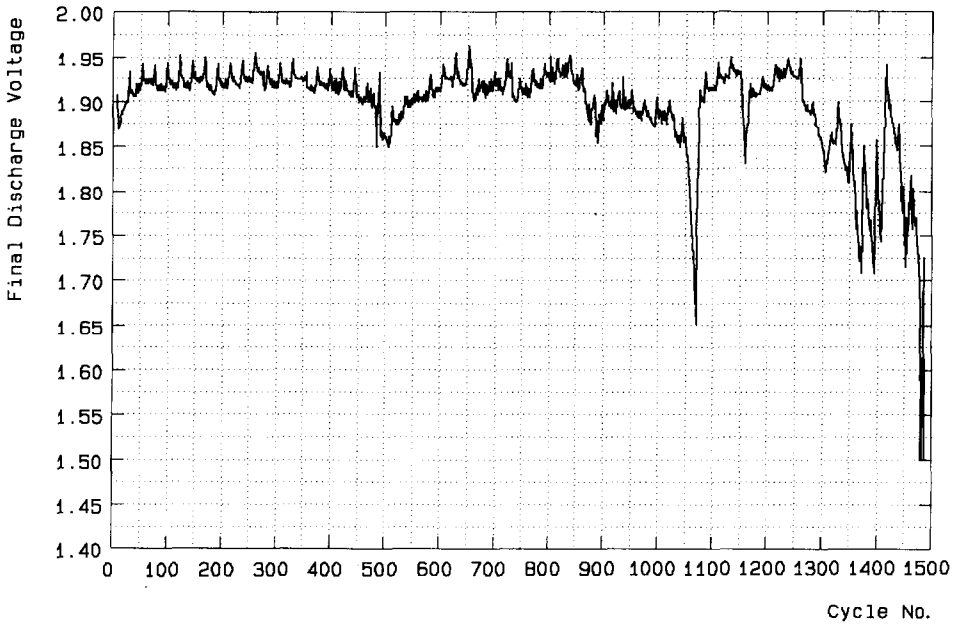

Fig. 3. Cycling of cell 9015 with free acid (flooded mode) 20 *C*/2.5 discharges to 50 Ah per kg positive mass + 3 *C*/5 discharges to 1.7 V. Only final voltage at 50 Ah per kg positive mass is shown (*C*/2.5 current).

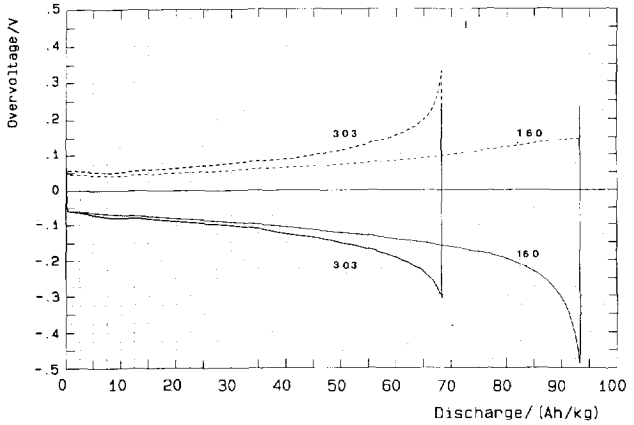

Fig. 4. Overvoltages for positive and negative plates during C/2.5 discharge of cell 9020 at cycles 160 and 303. (– – –) negative, (——) positive plate. Cycle numbers indicated at curves.

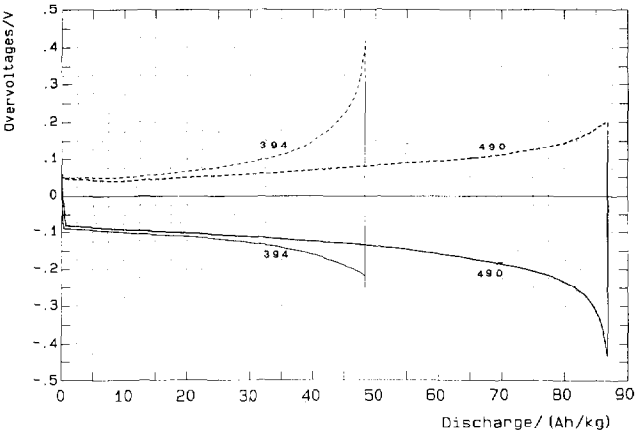

Fig. 5. Overvoltages for positive and negative plates during C/2.5 discharges of cell 9020 at cycle 394 (recombination) and cycle 490 (flooded mode). (– – –) negative, (——) positive plate. Cycle numbers indicated at curves.

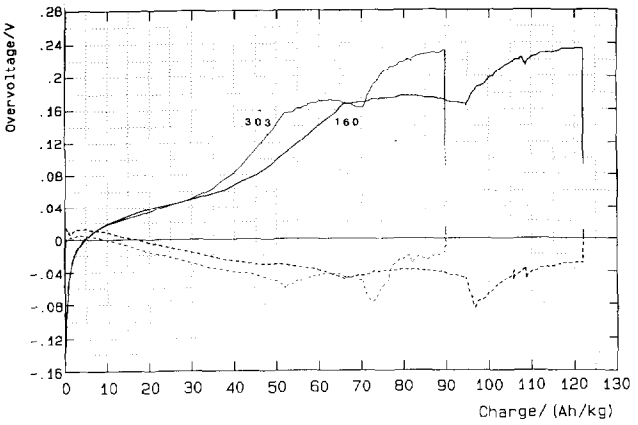

Fig. 6. Overvoltages for positive and negative plates during charge of cell 9020 at cycles 160 and 303. (– – –) negative, (——) positive plate. Cycle numbers indicated at curves. Charge profile 'IUI'.

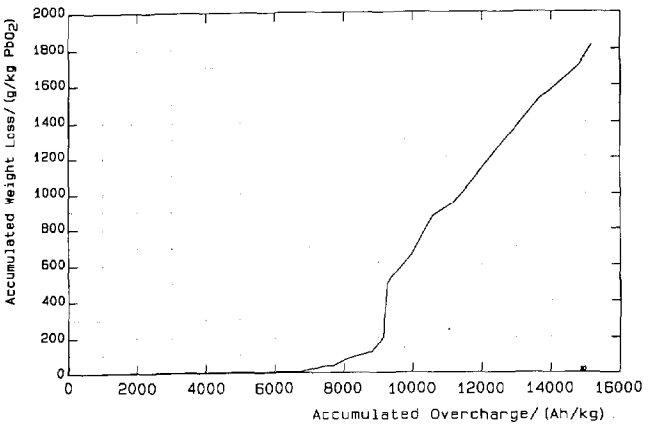

Fig. 7. Accumulated weight loss in g per kg positive mass vs. accumulated overcharge in Ah per kg positive mass for cell 9020 until cycle 900. Conversion to flooded mode at 8000 Ah per kg positive mass overcharge.

degradation of the negative is even more pronounced in cycle 394 shown in Fig. 5. The same picture was found for cell 9023.

The overvoltages during charging are shown in Fig. 6, which demonstrates that recombination works the same way in both cycles.

The failure of the negatives in the cells 9020 and 9023 is apparently due to sulfation (this term is used here to indicate that after charge the plate contains $PbSO_4$ that is not recharged).

This failure mode has been discussed recently [17] but it was considered as unimportant. However Sun et al. [18] have demonstrated a correlation between decreasing capacity and increasing $PbSO_4$ content in the charged negative plate.

To offset the failure, a number of different charging procedures was used, but with no effect. In cell 9015, with free acid, the negatives were subjected to the same pressure and cycling conditions and they did not show any signs of sulfation. It was then concluded, that the failure might be due to the recombination process. To prove this, the cells were converted to operation in the flooded mode, by adding water at cycle 400 until the separator was saturated with acid and a layer of 3 to 5 mm was present at top of the cell. The degree of recombination was observed by following the weight loss as a function of overcharge. This is shown in Fig. 7, where accumulated weight loss is shown as function of accumulated overcharge. Until water was added, recombination was virtually complete as demonstrated by zero weight loss. When the separator was saturated, the cell begins slowly to lose water by overcharge and from cycle 500, corresponding to 9200 Ah per kg PbO_2 accumulated overcharge, the water loss is proportional to overcharge. The slope is about 80% of the stoichiometric slope, showing that recombination is not completely absent, but reduced to about 20%.

At cycle 490 the negative has regained its full capacity as shown by the overvoltages depicted in Fig. 5. The cycling performance when the cell was operated in the

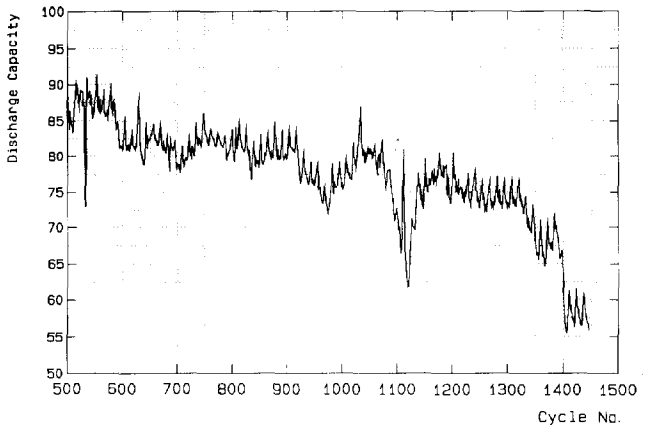

Fig. 8. Cycling of cell 9020 in the flooded mode. Discharge and charge as in Fig. 1. Only capacities at the *C*/2.5 discharges are shown.

flooded mode, is shown in Fig. 8 demonstrating that the cell performs satisfactorily at least to cycle 1400, as did the cell with free acid (9015). Operated this way cell 9020 delivered an accumulated capacity of 115 000 Ah per kg positive mass.

4. A recharge model

The failure of the negative when operated in the recombination mode is caused by an insufficient recharge in each cycle, causing an increasing degree of sulfation. When the surplus negative capacity, which is present initially, is converted to $PbSO_4$ which remains unconverted at the end of charge, the negative becomes capacity limiting.

There is an extensive literature treating the chemistry of recombination on overcharge, viz., the processes when both electrodes are fully charged and no $PbSO_4$ is present, see Refs. [13,19]. However, no comprehensive treatment of the role of recombination during recharge has been published.

The problems during recharge can be illustrated by considering the situation for the negative plate when the positive plate is fully charged and all the oxygen evolved at the positive is transported to the negative. In this case, all current to the negative is used for reduction of this oxygen since at the potential of the negative during charging the overvoltage for reducing oxygen is much more negative (about −2 V) than the overvoltage for the other possible cathodic reaction: lead deposition (−0.1 to −0.2 V). Thus, further charge of the negative becomes impossible. Consequently in this case, maintaining full capacity of the negative requires that the negative is always fully recharged before the positive.

In the flooded cell no such a situation can happen because the charging of the two electrodes proceeds independently.

The lack of balance between the two electrodes during recharge originates from the parasitic currents connected with hydrogen evolution at the negative and oxygen evolution at the positive.

As long as both plates contain $PbSO_4$, the reactions and associated partial currents are:

(i) at the negative:

$$PbSO_4 \Rightarrow Pb \qquad i_{Pb} \tag{1a}$$

$$H_2O \Rightarrow H_2 \qquad i_H \tag{1b}$$

$$O_2 \Rightarrow H_2O \qquad i_R \tag{1c}$$

(ii) at the positive:

$$PbSO \Rightarrow PbO_2 \qquad i_{PbO_2} \tag{2a}$$

$$H_2O \Rightarrow O_2 \qquad i_O \tag{2b}$$

The possible hydrogen oxidation at the positive is not included, as this process only occurs at a very small rate. If the total charging current is I, then:

$$I = i_{Pb} + i_H + i_R = i_{PbO_2} + i_O \tag{3}$$

The charges added to the negative and positive electrodes are respectively:

$$q_n = \int_0^t (I - i_H - i_R)\, dt \tag{4a}$$

$$q_p = \int_0^t (I - i_O)\, dt \tag{4b}$$

where t is the time on charge.
If:

$$\int_0^t (i_H + i_R)\, dt > \int_0^t (i_O)\, dt \tag{5}$$

then the negative is not completely recharged when the positive is fully charged and sulfation may occur. A similar relation was proposed previously [20].

In the recharge phase both plates work as mixed electrodes with the electrochemical Eqs. (1a)–(1c) and Eqs. (2a)–(2b) proceeding in parallel as expressed in Eq. (3). In this situation the partial currents are controlled by the overvoltages of the corresponding reactions with the electrochemical rate constants as parameters. To a lesser degree also transport parameters and the active electrode surface influence the currents.

During most of the recharge, the electrode potentials and thus the overpotentials for the parasitic reactions are controlled by Eqs. (1a) and (2a) as their rate constants are big compared with the rate constants for hydrogen and oxygen evolution. Near the end of recharge, however, when only small amounts of $PbSO_4$ are present, diffusion of Pb^{2+} becomes rate determining [21,22]. This results (at constant current) in an increase

in the single electrode potentials and the overpotentials for Eqs. (1b) and (2b).

Concerning the oxygen reduction current i_R at the negative electrode, the overpotential is that much negative, that it proceeds in the limiting current region and all oxygen arriving to the negative is reduced. Thus, this current is controlled by the transport conditions mainly through the separator. If γ is the fraction of oxygen transported to the negative, we have:

$$i_R = \gamma i_O \tag{6}$$

where γ is the recombination efficiency.

Eqs. (1b) and (2b) have also large overvoltages: -0.4 to -0.6 V and 0.5 to 0.6 V, respectively. They work in the Tafel region [23,24] where the current is exponentially dependent on overvoltage. The rate constants are small in particular for hydrogen evolution.

In the following a crude linear approximation is used for the currents i_H and i_O in the recharge region. It is assumed that they are zero up to a certain degree of recharge and then constitute a constant fraction of the charge current. There is some justification for this model in the practical observations that gas evolution is near zero in the beginning and first becomes important when a certain degree of charge is reached [25].

It is convenient to formulate the proposed model in terms of the states of recharge, s_+ and s_- for the positive and negative plate, respectively:

$$s_- = 1/q_d\left(\int_0^t i_{Pb}\,dt\right) \tag{7a}$$

$$s_+ = 1/q_d\left(\int_0^t i_{PbO_2}\,dt\right) \tag{7b}$$

where q_d is the capacity delivered during the preceding discharge.

If s_O is the state of recharge where oxygen evolution begins and β the fraction of current used for oxygen evolution the model for the recharge of the positive plate is:

$$s_+ < s_O \qquad i_{PbO_2} = I \tag{8a}$$

$$s_O < s_+ < 1 \qquad i_{PbO_2} = (1-\beta)I \tag{8b}$$

$$s_+ = 1 \qquad i_{PbO_2} = 0 \tag{8c}$$

The corresponding parameters for hydrogen evolution are s_H and α. It is a common observation [26] that oxygen evolution starts before hydrogen evolution (the rate constant for hydrogen evolution is much smaller) thus $s_H > s_O$. Taking the current used for recombination into consideration and at sufficient recombination efficiency, the model for the negative is:

$$s_- < s_O \qquad i_{Pb} = I \tag{9a}$$

$$s_O < s_- < s_H \qquad i_{Pb} = (1-\beta\gamma)I \tag{9b}$$

$$s_+ = 1;\ s_H < s_- < s^* \qquad i_{Pb} = (1-\alpha-\beta\gamma)I \tag{9c}$$

where s^* is the value of s_- when the positive is fully charged.

If $(\alpha+\gamma)<1$ then:

$$s_+ = 1;\quad s^* < s_- < 1 \qquad i_{Pb} = (1-\alpha-\gamma)I \tag{9d}$$

however if $(\alpha+\gamma)>1$, then recharge of the negative above s^* is impossible.

Modification of this model for the case of low or no recombination is obvious.

The state of recharge can be found by integration as functions of the charge factor, c, defined as:

$$c = 1/q_d\left\{\int_0^t I\,dt\right\} \tag{10}$$

Then for the positive:

$$s_+ < s_O \qquad s_+ = c \tag{11a}$$

$$s_O < s_+ < 1 \qquad s_+ = (1-\beta)c + \beta s_O \tag{11b}$$

which gives the charge factor for $s_+ = 1$:

$$c_+ = \frac{1-\beta s_O}{1-\beta} > 1 \tag{12}$$

If the charge factor for $s_- = s_H$ is c_H, then for the negative:

$$s_- < s_O \qquad s_- = c \tag{13a}$$

$$s_O < s_- < s_H \qquad s_- = (1-\beta\gamma)c + \beta\gamma s_O \tag{13b}$$

$$\text{if } s^* < 1;\quad s_H < s_- < s^* \qquad s_- = (1-\alpha-\beta\gamma)(c-c_H) + s_H \tag{13c}$$

c_H can be found from:

$$c_H = \frac{s_H - \beta\gamma s_O}{1-\beta\gamma} \tag{14}$$

If recombination is sufficiently small, the negative may get fully recharged before the positive. In this case, we may get a charge factor, c_-, for $s_- = 1$:

$$c_- < c_+ \qquad c_- = c_H + \frac{1-s_H}{1-\alpha-\beta\gamma} \tag{15}$$

If the positive is recharged at first, the critical value for the state-of-charge of the negative may be found from:

$$s^* = s_H + (1-\alpha-\beta\gamma)(c_+ - c_H) \tag{16}$$

With complete recombination, $\gamma = 1$, the loss in negative recharge in each cycle: $1-s^*$ is:

$$\Delta = 1 - s^* = \frac{\alpha}{1-\beta}(1-s_H) \tag{17}$$

In the case of $\alpha+\gamma<1$, recharge of the negative can continue beyond c_+. The charge factor necessary to obtain full recharge is then:

$$c_-^* = c_+ + \frac{1-s^*}{1-\alpha-\gamma} \tag{18}$$

As demonstrated below this charge factor may be prohibitively large.

The contents of the above equations are illustrated in Figs. 9 to 11, where the states of recharge, s_+ and s_-, are depicted against the charge factor c. The parameters α, β, γ and s_O and s_H are chosen somewhat at random in order to illustrate the important points in the recharge theory. The oxygen-evolution parameters are estimated from data in the literature [26,27], whereas the hydrogen evolution is overestimated for a virgin (not cycled) plate.

In Fig. 9, the recharge for the positive and for the negative for complete recombination ($\gamma=1$) and for partial recombination ($\gamma=0.75$) is shown. It is seen that the positive attains full charge first. For $\gamma=1$, the negative can only be recharged to 90% of the preceding discharge, whereas for $\gamma=0.75$ full recharge can be obtained, but only at an unpractical overcharge of 70%.

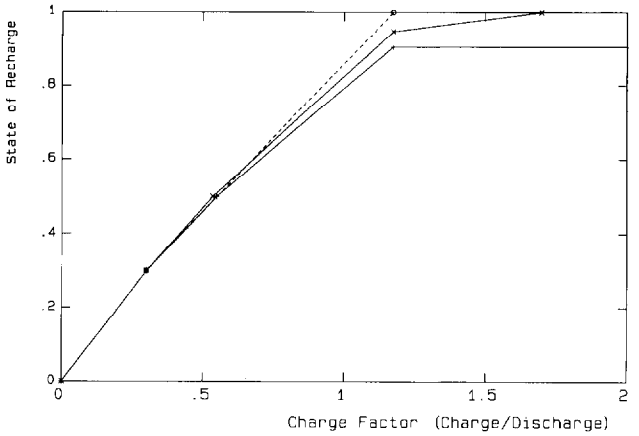

Fig. 9. Calculated state of recharge vs. charge factor for (– – –) positive and (——) negative electrode. Parameters used: $s_H=0.5$, $\alpha=0.15$, $s_O=0.3$, $\beta=0.2$, $\gamma=0.75$ (×) and 1.0 (+).

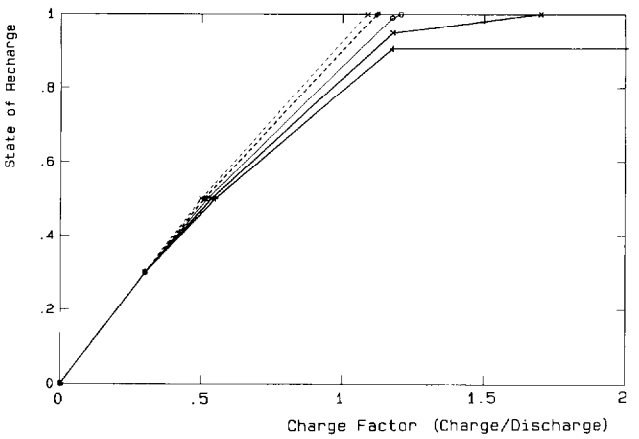

Fig. 10. Calculated state of recharge vs. charge factor for negative plate at different degrees of recombination. (– – –) and (+) $\gamma=0$; (– – –) and (*) $\gamma=0.25$; (——) and (□) $\gamma=0.5$; (——) and (×) $\gamma=0.75$; (——) and (+) $\gamma=1$. Other parameters as in Fig. 9.

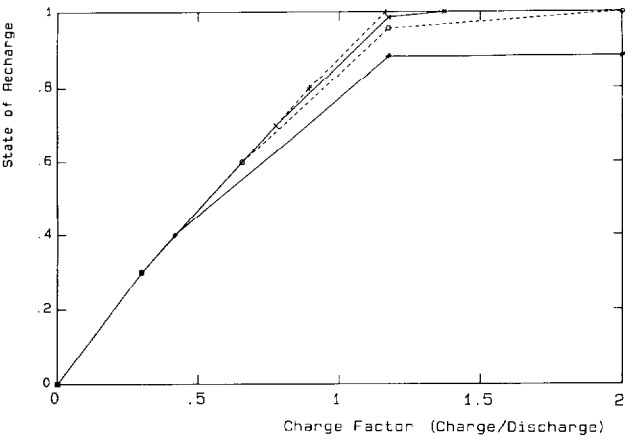

Fig. 11. Calculated state of recharge vs. charge factor for negative plate at different hydrogen-evolution rates. α/s_H: (– – –) and (+) 0.1/0.8; (——) and (×) 0.125/0.7; (– – –) and (□) 0.15/0.6; (——) and (*) 0.2/0.4. Other parameters: $\gamma=0.8$; $s_O=0.3$, $\beta=0.2$.

In Fig. 10, the effect of varying the recharge efficiency is demonstrated. With the parameters used, reasonable recharge is obtained for $\gamma<0.5$.

Eq. (17), even if valid only for $\gamma=1$, points to the dominating influence of the hydrogen-evolution rate. Fig. 11 shows how, for a reasonable value of recombination: $\gamma=0.8$, the hydrogen-evolution parameters influence the recharge possibilities.

5. Discussion

It may be argued that the model used above for the partial currents is too crude to describe the recharge process. But simple qualitative arguments, independent of the model, give, in limiting cases, the same results.

The model is intended for a systematic approach to a description of the way the critical factors, hydrogen evolution and recombination efficiency, influence the recharge of the negative plate. When, as in sealed and valve-regulated batteries, a high recombination efficiency is desired even a small amount of hydrogen evolution may cause insufficient recharge of the negative plate.

As the accumulated loss of capacity is proportional to the depth-of-discharge and the number of cycles, this loss may be of minor importance in applications where only shallow cycles or a few deep cycles are required. However, if as in motive power applications the demand is 1000 to 1500 deep cycles a recharge efficiency above 99.9% is necessary.

The decrease in negative capacity can be partially counteracted by designing the cell with a large excess of negative mass, which is mostly done to facilitate recombination. But this is of little help as the insufficient recharge leaves unconverted $PbSO_4$ which reduces the amount of acid. As recombinant cells are often designed with a minimum of acid, this loss may be critical depressing the positive capacity and the cell voltage.

The rate of hydrogen evolution depends primarily on the purity of the spongy lead in the negative. Deposition of impurities as, e.g., antimony may increase the hydrogen-evolution rate considerably. For this reason, the grid alloy used for the positive plate is a critical factor. If an antimony alloy is used, corrosion of the positive grid during long-term cycling will liberate antimony, which eventually is deposited in the negative plate [28–31]. This makes control of hydrogen evolution extremely difficult.

To get a quantitative estimate of this effect, Tafel curves for hydrogen evolution on the negative plate of cell 9020 after 1600 cycles were measured and compared with hydrogen evolution on a not cycled plate. These curves are shown in Fig. 12. Estimates of the rate constants show that during cycling the rate constant for hydrogen evolution has increased by a factor of at least 100. This explains why continued operation of the cell in the recombination mode was impossible.

Thus, due to grid corrosion the use of antimonial grids for the positive electrode appears to be extremely critical. A possible remedy may be the addition of inhibitors for hydrogen evolution [31].

Lead–calcium alloys have been used for the negative to suppress hydrogen evolution on this grid. These alloys may be a possibility also for the positive grid, but there is some uncertainty as to the reliability of the positive plate with non-antimonial grids. Fortuitous failure apparently occurs at some cycling conditions [17,32] even if the addition of a tin coating appears advantageous [33].

It is also reported that in combination with a compressed absorptive glass mat separator these failures are less frequent. Anyhow, VRLA batteries built this way are reported to deliver up to 1000 cycles with an 80% depth-of-discharge [34,35].

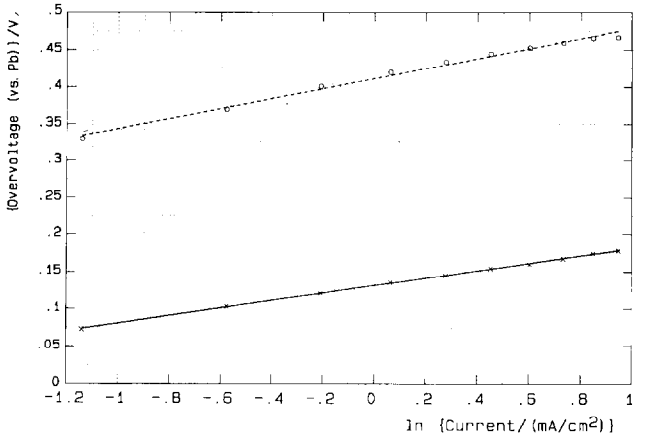

Fig. 12. Tafel plots for hydrogen evolution on (– – –) virgin and (——) cycled negative plate in 1.28 sp. gr. H_2SO_4. Overvoltages/V (relative to Pb rest potential) vs. ln(current/mA cm^{-2}).

6. Conclusions

From the literature one gets the impression that the main reason for suppressing hydrogen evolution is the need to avoid water loss in valve-regulated cells or to prevent excessive internal pressure in sealed cells [36,37]. This may apply to stand-by and shallow cycling applications.

The present work points to the fact that hydrogen evolution in combination with a high recombination efficiency may cause loss of negative capacity and sulfation, thus impeding the possibility of obtaining a large number of deep cycles.

In order to minimize hydrogen evolution, antimony-free grids both for the positive and the negative are recommended. However, deep cycling of batteries with antimony-free positive grids may present problems for the positive plate. Even with such grids a small amount of hydrogen evolution or corrosion of the negative by oxygen from the outside may still occur.

For these reasons it has been stated that 'oxygen recombination is clearly desirable to some extent, but it is becoming clear that only a moderate level of recombination may be optimal for these systems' [38].

The present work supports this point of view, and aims at providing an approach to choose the best balance between projected cycle life, recombination efficiency and measures to minimize hydrogen evolution.

List of symbols

c	recharge factor, defined in Eq. (10)
c_+	recharge factor for full recharge of positive plate, defined in Eq. (12)
c_-	recharge factor for negative plate when fully rechargeable, defined in Eq. (15)
c_-^*	recharge factor, when negative can be recharged after full charge of positive, defined in Eq. (18)
c_H	recharge factor for negative when hydrogen evolution begins
I	charge current
i_H	partial current for hydrogen evolution at negative
i_{Pb}	partial current for lead deposition
i_{PbO_2}	partial current for PbO_2 formation
i_O	partial current for oxygen evolution at positive

i_R partial current for oxygen reduction at negative
q_d charge delivered during preceding discharge
q_n charge accepted by negative, defined in Eq. (4a)
q_p charge accepted by positive, defined in Eq. (4b)
s_- state of recharge of negative, defined in Eq. (7a)
s_+ state of recharge of positive, defined in Eq. (7b)
s_H state of recharge of negative, when hydrogen evolution begins
s_O state of recharge of positive, when oxygen evolution begins
s^* state of recharge of negative, when positive is fully charged, assumed that $s_- < 1$; defined in Eq. (16)
t recharge time (s)

Greek letters

α proportionality factor for hydrogen evolution at negative
β proportionality factor for oxygen evolution at positive
γ recombination efficiency

References

[1] J.F. Cole, *J. Power Sources, 40* (1992) 1–5.
[2] J.M. Stevenson and J.L. Dyson, *J. Power Sources, 40* (1992) 39–40.
[3] J. Alzieu and J. Robert, *J. Power Sources, 13* (1984) 93–100; J. Alzieu, N. Koechlin and J. Rober, *J. Electrochem. Soc., 144* (1987) 1881–1884.
[4] S. Atlung and B. Zachau-Christiansen, *Long Life Lead–Acid Cells with Pasted Positive Plates,* Rep. to the Danish Department of Energy, 1992, available from Risø National Laboratories.
[5] J. Garche, E. Voss, R.F. Nelson and D.A.J. Rand, *J. Power Sources, 36* (1991) 405–413.
[6] S. Atlung and B. Zachau-Christiansen, *J. Power Sources, 30* (1990) 131–141.
[7] J. Kim, S.H. Oh and H.Y. Kang, in T. Keilly and B.W. Baxter (eds.), *Power Sources 13,* International Power Sources Symposium Committee, Leatherhead, UK, 1991, pp. 71–80.
[8] R.J. Szper, *Proc. Int. Symp. Batteries, Christchurch, New Zealand, 1958,* Paper X.
[9] K. Yonczu, M. Tsubota and K. Takahashi, *US Patent No. 4 336 314* (1982).
[10] K. Takahashi, M. Tsubota, K. Yonezu and K. Ando, *J. Electrochem. Soc., 130* (1983) 2144–2149.
[11] D.A. Crouch and J.W. Reitz, *J. Power Sources, 31* (1990) 125–134.
[12] B. Culpin and J.A. Hayman, in L.J. Pearce (ed.), *Power Sources 11,* International Power Sources Symposium Committee, Leatherhead, UK, 1987, pp. 45–67.
[13] R.F. Nelson, *J. Power Sources, 31* (1990) 3–23.
[14] S. Warrel, *J. Power Sources, 31* (1990) 35–42.
[15] S.V. Jensen and O.G. Nissen, *8 Int. Electrical Vehicle Symp.,* Oct. 1986, Washington, DC, USA.
[16] K. Peters, *J. Power Sources, 43* (1993) 155–164.
[17] B. Culpin and D.A.J. Rand, *J. Power Sources, 36* (1991) 415–438.
[18] Y.-M. Sun, G.-D. Li, Q.-Y. Hao and M. Chang, in T. Keilly and B.W. Baxter (eds.), *Power Sources 13,* International Power Sources Symposium Committee, Leatherhead, UK, 1991, pp. 71–81.
[19] J. Mrha, J. Jindra and M. Musilova, *J. Power Sources, 32* (1990) 303–312.
[20] J.S. Symanski, B.K. Mahato and K.R. Bullock, *J. Electrochem. Soc., 135* (1988) 548–551.
[21] P. Ekdunge and D. Simonson, *J. Electrochem. Soc., 132* (1985) 2521–2529.
[22] P. Ekdunge, K.V. Rybalka and D. Simonson, *Electrochim. Acta, 32* (1987) 659–667.
[23] M. Barak, M.I. Gillibrand and D.R. Lomax, *Proc. Int. Symp. on Batteries, Christchurch, New Zealand, 1958, Paper M.*
[24] P. Ruetschi, R.T. Angstadt and B.D. Cahan, *J. Electrochem. Soc., 106* (1959) 547–551.
[25] W.G. Sunu and B.W. Burrows, in J. Thompson (ed.), *Power Sources 8,* Academic Press, New York, 1981, pp. 601–619.
[26] W. Wisscher, in L.J. Pearce (ed.), *Power Sources 10,* International Power Sources Symposium Committee, Leatherhead, UK, 1985, pp. 525–535.
[27] A.M. Hardman, *J. Power Sources, 23* (1988) 127–134.
[28] J.L. Dawson, M.I. Gillibrand and J. Wilkinson, in D.H. Collins (ed.), *Power Sources 3,* Oriel Press, Newcastle upon Tyne, 1971, pp. 1–12.
[29] B. Berndt and S.C. Nijhavan, *J. Power Sources, 1* (1976/77) 3–15.
[30] A.A. Jenkins, W.C. Maskell and F.L. Tye, *J. Power Sources, 19* (1987) 75–80.
[31] W. Böhnstedt, C. Radel and F. Scholten, *J. Power Sources, 19* (1987) 303–314.
[32] J. Manders, *J. Power Sources, 38* (1992) 197–227.
[33] B. Culpin, A.F. Hollenkamp and D.A.J. Rand, *J. Power Sources, 38* (1992) 63–74.
[34] C. Böhle and R. Kiessling, *J. Power Sources, 31* (1990) 145–150.
[35] E. Nann, *J. Power Sources, 33* (1991) 93–103.
[36] J. Mrha, K. Micka, J. Jindra and M. Musilova, *J. Power Sources, 27* (1989) 91–117.
[37] H. Dietz, M. Radwan, H. Döhring and K. Wiesner, *J. Power Sources, 42* (1993) 89–101.
[38] R.F. Nelson, in T. Keilly and J. Baxter (eds.), *Power Sources 13,* International Power Sources Symposium Committee, Leatherhead, UK, 1991, pp. 13–24.